ISIJ International, Vol. 57 (2017), No. 10, pp. 1703–1709

Rate of $2CaO{\cdot}SiO_2$ Dissolution into Molten CaO–FeO–SiO_2 Slag Saturated with Solid Iron

Yoshinao KOBAYASHI[1)]* and Takahide SADAMOTO[2)]

1) Institute of Innovative Research, Tokyo Institute of Technology N1-3, 2-12-1, Ookayama, Meguro-ku, Tokyo, 152-8550 Japan. 2) Graduate Student, Tokyo Institute of Technology. Now at Nippon Steel & Sumitomo Metal Corporation, 1 Oaza-Nishinosu, Oita-shi, Oita, 870-0992 Japan.

(*Received on June 8, 2017; accepted on August 9, 2017*)

Rate of $2CaO{\cdot}SiO_2$ dissolution into molten CaO–FeO–SiO_2 slag saturated with solid iron has been investigated considering the promotion of lime fluxing. A new diffusion couple method has been applied where $2CaO{\cdot}SiO_2$ pellet was immersed into molten CaO–FeO–SiO_2 slag in an iron crucible, slag convection being suppressed. Concentration profile of components was observed and the diffusion behavior was well understood. Considering the pseudo-binary inter-diffusion between components such as CaO and SiO_2 and slag phase matrix, diffusivity of CaO and SiO_2 in the present slag has been determined to have the values from 4.9×10^{-7} to 4.7×10^{-5} cm^2/s at temperatures from 1 573 to 1 673 K. Assuming the dissolution mechanism as continuous formation and dissolution of $2CaO{\cdot}SiO_2$ on the surface of CaO, complete dissolution time into the flowing slag has been estimated on the basis of the Ranz-Marshall empirical equation, and temperature is found to be controlling factor of the dissolution rate in the normal operation condition.

KEY WORDS: lime; CaO; $2CaO{\cdot}SiO_2$ dissolution; rate; diffusivity.

1. Introduction

A growing attention has been paid for the promotion of lime fluxing in order to meet the recent demands, that is, high efficiency and rapid operation of refining processes, which realize reduction of slag emission and suppression of calcium fluoride as well as shortening the operation time. Up to now, there have been several investigations reported on the dissolution behaviour of CaO into refining slags. Matsushima *et al.*[1)] have shown the appropriateness to take the difference between CaO concentration of the slag and that for CaO saturation as the driving force of the CaO dissolution into the slag. Recently, the effect of additional components such as Al_2O_3 and CaF_2 on the dissolution rate of CaO into the CaO–Fe_tO–SiO_2 slag has been investigated.[2)] Regarding the multi–phase flux refining process,[3)] absorption of phosphorus into $2CaO{\cdot}SiO_2$ phase (hereafter, abbreviated as "C2S") has been elucidated. Innovative work has been done on the utilization of gas generation from the quick lime which effectively crushes the surface layer to promote the CaO dissolution.[4)]

Mechanism of CaO dissolution which has been revealed on the basis of the foregoing studies is that C2S layer firstly forms on the surface of the lime on immersion and then dissolves into slag rich in FeO, where two steps reactions are considered and the rate–controlling step would be the C2S dissolution into molten slag.[5)] However, all these investigations were made by using CaO as the starting material, not C2S. Regarding mass transfer of each oxide component in the slag, many studies have been reported in viewpoint of diffusivity, namely, tracer diffusivity of Fe in the CaO–FeO–SiO_2 system,[6)] pseudo-binary inter-diffusivity of CaO–SiO_2 and CaO–Al_2O_3 in the CaO–Al_2O_3–SiO_2 system obtained by the electric current method,[7)] evaluation of inter-diffusivity from tracer diffusivity[8)] and that of pseudo-binary inter-diffusivity derived from viscosity in the CaO–FeO–SiO_2 system as well as that of diffusion paths considering up-hill diffusion.[9)] Liquid phase diffusion couple methods follow the above investigation where pseudo-binary inter-diffusivities have been revealed in the $20Fe_2O_3$-35CaO-45SiO_2 system on mass% basis[10)] and those of impurities have been reported for the CaO–Al_2O_3–SiO_2 and Fe_2O_3–CaO–SiO_2 systems[11)] However, diffusivities for the iron saturated Fe_tO–CaO–SiO_2 system have not been established.

On the basis of these backgrounds, the present study aims to investigate the dissolution behaviour of C2S into the CaO–Fe_tO–SiO_2 slag saturated with solid iron and consequently to evaluate the pseudo-binary apparent diffusivity in this system. Through the estimation of the complete dissipation time of C2S sphere in the slag considering the effect of slag flow rate, the controlling factors of the CaO dissolution rate have been discussed.

* Corresponding author: E-mail: kobayashi.y.at@m.titech.ac.jp
DOI: http://dx.doi.org/10.2355/isijinternational.ISIJINT-2017-328

2. Experimental

2.1. Preparation of Samples

Raw material for the present slag was a mixture of CaO calcined from $CaCO_3$ (99.9% in purity), SiO_2 powder (99.9% in purity), and Fe_tO precedently prepared by melting Fe (99.99% in purity) and Fe_2O_3 (99% in purity) powder in an iron crucible. **Table 1** gives nominal composition of the slag and **Fig. 1** shows these compositions plotted on the CaO–FeO–SiO_2 ternary system.[12] After complete mixing, the powders were melted in an iron crucible for 1 h at 1 673 K in an argon atmosphere. After taking out and quenching the sample, it was subjected to the main experiments.

Raw material for the C2S was a mixture of CaO calcined from $CaCO_3$ (99.9% in purity), SiO_2 powder (99.9% in purity), and $3CaO{\cdot}P_2O_5$. Since preparation of stable C2S pellet is very difficult, binding component of P_2O_5 was added by 5 mass% using $3CaO{\cdot}P_2O_5$. The molar ratio of CaO to SiO_2 was arranged to be 2 on the basis of the stoichiometric composition. The mixture powder was heated up to 1 673 K and held for 24 h in the air, followed by cooling in argon gas flow. Then, the powder was mixed again and compressed into the cylinder shape by a die assembly having the diameter of 20 mm at 100 MPa for a holding time of 2 min, followed by the sintering at 1 673 K for 24 h in the air and cooling in argon gas flow. The sample was checked by XRD analysis to confirm the formation of C2S. This sintered compact was machined to have the cylindrical shape having the diameter of 5 mm or rectangular parallelepiped shape having the dimension of 4.5×4.5×12 mm, which was attached to the tip of the mullite tube having the diameter of 8 mm, and subjected to the main experiments. Iron crucibles used in the present experiment were made of iron rods to have a hole with the diameter of 8 mm.

Table 1. Chemical composition of slags (mass%).

	CaO	SiO_2	FeO	CaO/SiO_2
Slag A	30	50	20	0.6
Slag B	20	40	40	0.5
Slag C	21.6	28.4	50	0.76
Slag D	13.3	6.7	80	1.99

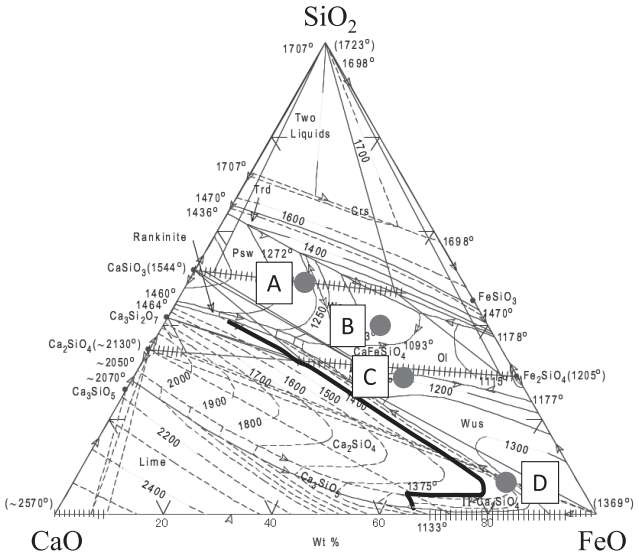

Fig. 1. Composition of slags on the CaO–FeO–SiO_2 phase diagram.[12]

2.2. Experimental Procedure

A new diffusion couple method has been developed in the present work, where diffusion behavior between liquid and solid phase can be well figured out. A C2S sample prepared by the preceding manner was pre-heated to reach the temperature almost the same as the melted slag by placing just above the iron crucible in the electric resistance furnace and immersed into the iron crucible containing pre-melted slag which was prepared in the foregoing fashion. The possible convection in the molten slag during the experiment would be significantly suppressed since the clearance between the C2S phase and iron crucible wall was ranging from 0.5 to 1 mm approximately and narrow enough. The iron crucible was suspended by Kanthal wire of 23Cr-69Fe-6Al during this immersion experiment. After the intended holding time ranging from 3 to 60 s, the wire was cut and the iron crucible was vertically dropped in the furnace tube and quenched into the water in a bucket placed just below the furnace. This method can avoid possible fluctuation and movement of the slag in the crucible during solidification. The experiment conditions are listed in **Table 2**.

2.3. Sample Analysis

After quenching the sample, the iron crucible was cut to show the cross section in the radial direction and submitted to the following analyses. The morphology of the interface between slag and C2S and concentration distribution of each element was analyzed by SEM-EDS (Scanning Electron Microscope with Energy Dispersive Spectroscopy). Line analysis was implemented in the radial or normal direction from the center of the cylinder or square column of C2S to the slag part as shown in **Fig. 2**.

Table 2. Experimental conditions.

shape of $2CaO{\cdot}SiO_2$	Cylinder				Rectangular Parallelepiped			
Slag compositions / Temperature/K	A	B	C	D	A	B	C	D
1 573	–	–	–	–	–	○	○	–
1 623	–	–	–	–	–	○	○	–
1 673	○	○	○	○	–	○	○	–
1 723	–	–	–	–	–	○	○	–

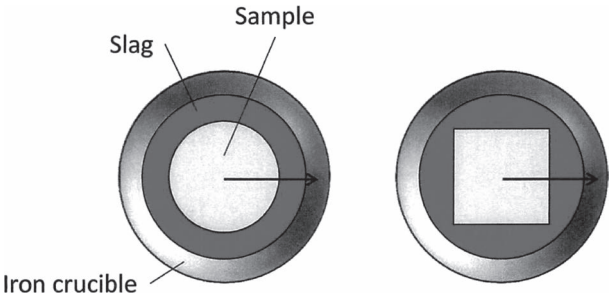

Fig. 2. Schematic diagram of samples with line analysis direction.

3. Results and Discussion

Figure 3 shows diffraction pattern as the result of XRD analysis on the as-sintered C2S samples. As was intended, the peaks of C2S and $3CaO{\cdot}P_2O_5$ phase were observed and formation of these phase was successfully confirmed. **Figure 4** shows the elemental map data in the vicinity of the interface between C2S and slag after the experiment with slag A held for 1 min at 1 673 K as a typical experimental result. Calcium diffused from C2S phase to slag phase while silicon and iron diffused the other way around, reflecting the initial concentration gap between C2S and slag for each element. **Figure 5** shows concentration profile of the components such as CaO, SiO_2, FeO and P_2O_5 for the samples of slag A, B, C, and D with cylindrical C2S held for 20 s at 1 673 K, respectively. **Figure 6** shows concentration profile of CaO, SiO_2, FeO and P_2O_5 for the samples of slag B and C with rectangular parallelepiped C2S held from 20 to 40 s at the temperature ranging from 1 573 to 1 673 K. Sintered C2S pellets often had cracks and defects, and some small portions were left out from the surface during polishing for the observation, which induces the scattering and fluctuation in the concentration profiles; however, the ratio of CaO/SiO_2 can be regarded kept to be 2 on the whole. On the other hand, CaO and SiO_2 concentrations show smooth gradient in the slag phase in the radial direction, which indicates that the dissolution reaction of C2S into the slag is controlled by mass transfer in the slag phase. Difficulty lies in the determination of the interface between C2S and slag phase after experiment; however, the portion showing steep gradient of concentration is thought to have been penetrated by liquid slag during experiments, the right edge of which portion is regarded as the interface. The region on the right hand side of this interface, namely the slag phase, was used for analyses to make kinetic discussion in viewpoint of concentration change with distance from the interface at given holding times.

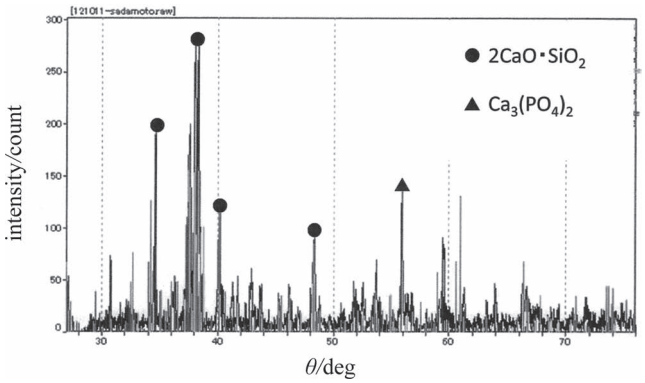

Fig. 3. X-ray diffraction pattern for as-sintered C2S sample.

In general, kinetic discussion on the diffusion should be made on the basis of the Onsager phenomenological diffusion equation which involves the chemical potential gradient of each component expressed by Eq. (1):

$$J_i = -M_{i1}(d\mu_1/dx) - M_{i2}(d\mu_2/dx) - \bullet\bullet\bullet \quad \text{..... (1)}$$

In the ternary system, Eq. (1) can be re-written for the first and second components as Eqs. (2) and (3) including diagonal terms of cross-effect.[13]

$$J_1 = -D^3_{1-1}(dC_1/dx) - D^3_{1-2}(dC_2/dx) \quad \text{..... (2)}$$

$$J_2 = -D^3_{2-1}(dC_1/dx) - D^3_{2-2}(dC_2/dx) \quad \text{..... (3)}$$

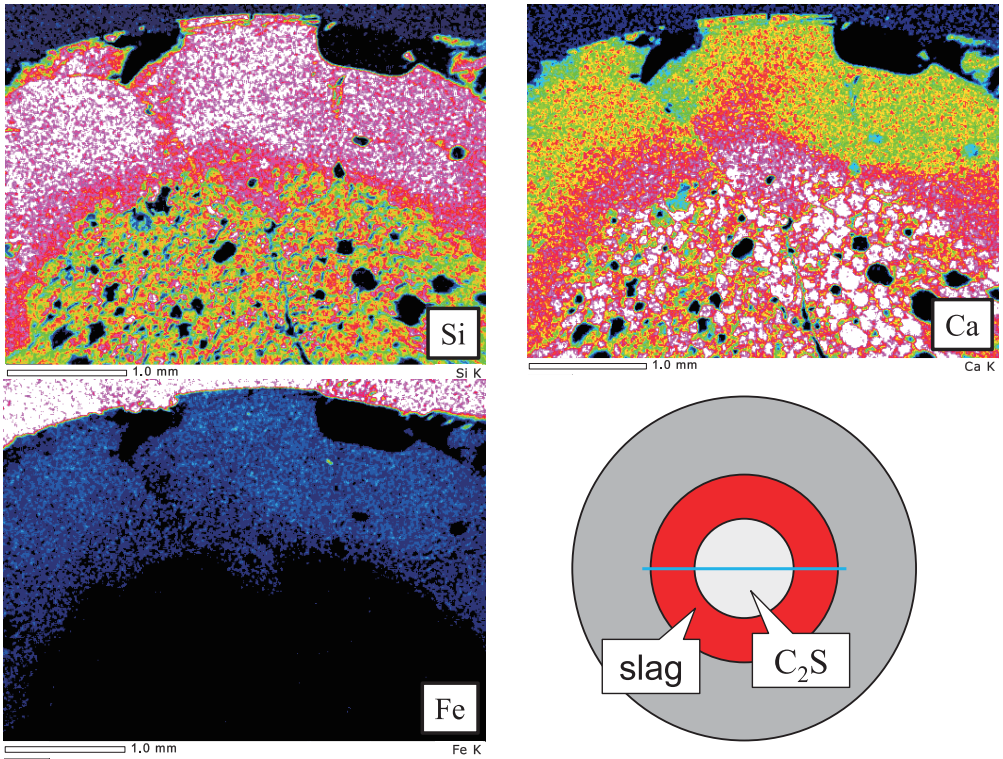

Fig. 4. Elemental mapping data in the vicinity of the interface between C2S and slag after the experiment at 1 673 K for 1 min.

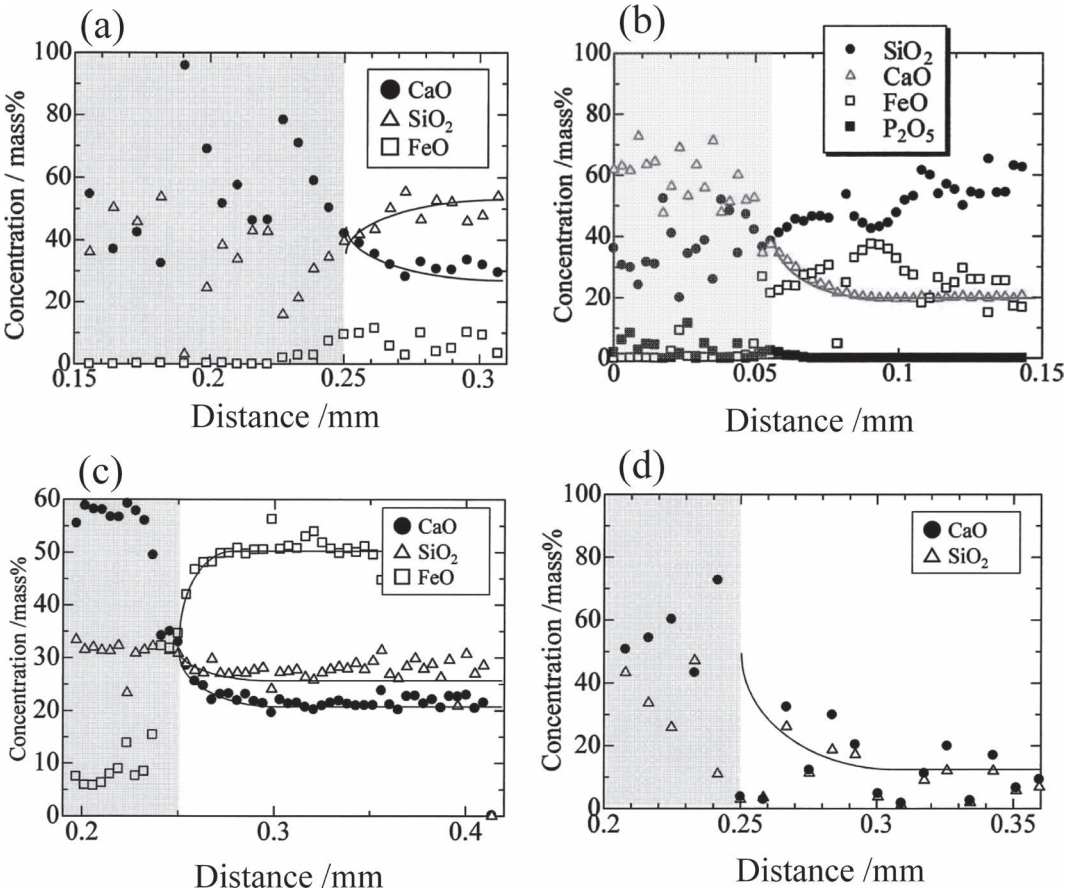

Fig. 5. Concentration profile for the components in the sample of (a) slag A, (b) slag B, (c) slag C and (d) slag D held for 20 s at 1 673 K.

where the subscript j–k, for example, 1-1, 1-2 and so on, denotes the sorts of diffusivity as transport coefficient for each term, and it is noted that concentration of j is independent variable and that of k is dependent variable. Thus, to determine D in this matrix, the diffusion couple experiments should be conducted so that the third component is kept constant in the compositional direction of diffusion path. However, the present system involves C2S and slag phases where any component would not be constant in the region of reaction interface between them. Hence, the apparent pseudo-binary inter-diffusivity has been considered in the present study, supposing that each component such as CaO and SiO_2 diffuses into slag matrix of the given composition.

The present systems can be analyzed on the basis of two types of un-steady one dimensional diffusion equations, namely, that for cylindrical and rectangular coordinate systems, respectively. The general case for the former is described in the cylindrical coordination of (r, θ, z) as follows;

$$\frac{\partial C}{\partial t}=\frac{1}{r}\left\{\frac{\partial}{\partial r}\left(rD\frac{\partial C}{\partial r}\right)+\frac{\partial}{\partial \theta}\left(\frac{D}{r}\frac{\partial C}{\partial \theta}\right)+\frac{\partial}{\partial z}\left(rD\frac{\partial C}{\partial z}\right)\right\} \quad \text{....(4)}$$

Supposing that substantial diffusion occurred only in the radial direction, Eq. (4) can be rewritten as Eq. (5).

$$\frac{\partial C}{\partial t}=\frac{1}{r}\frac{\partial}{\partial r}\left(rD\frac{\partial C}{\partial r}\right) \quad \text{.....(5)}$$

Assuming that diffusivity does not change since the change in slag composition is small and that the composition at far distance remains unchanged from initial state, the solution of the equation above is obtained as circular function expressed by Eq. (6).

$$\frac{C-C_0}{C_1-C_0}= 1+\frac{2}{\pi}\int_0^{\infty}\exp(-Du^2t)\frac{J_0(ur)Y_0(ua)-Y_0(ur)J_0(ua)}{J_0^2(ua)+Y_0^2(ua)}\frac{du}{u} \quad \text{....(6)}$$

$$J_\alpha=\sum_{m=0}^{\infty}\frac{(-1)^m}{m!\Gamma(\mathrm{m}+\alpha+1)}\left(\frac{x}{2}\right)^{2m+\alpha} \quad \text{.....(7)}$$

$$\mathrm{Y}_\alpha=\frac{J_\alpha(x)\cos(\alpha\pi)-J_{-\alpha}(x)}{\sin(\alpha\pi)} \quad \text{.....(8)}$$

$$\Gamma(x)=\int_0^{\infty}e^{-t}t^{x-1}dt \quad \text{.....(9)}$$

Fitting has been made on the concentration profile along with r at a given t by changing D, consequently to obtain the pseudo inter-diffusivity of D_{CaO} and D_{sio_2}. For the latter case of rectangular coordinate system, the solution of one-dimensional diffusion equation is rather simple and described as follows;

$$\frac{C-C_0}{C_1-C_0}=erfc\left(\frac{x}{2\sqrt{Dt}}\right) \quad \text{.....(10)}$$

On the basis of these solutions for two types of coordinates corresponding to each experimental set-up, diffusivities, D_{CaO}, D_{sio_2} in the slag A, C, and D at 1 673 K listed in **Table**

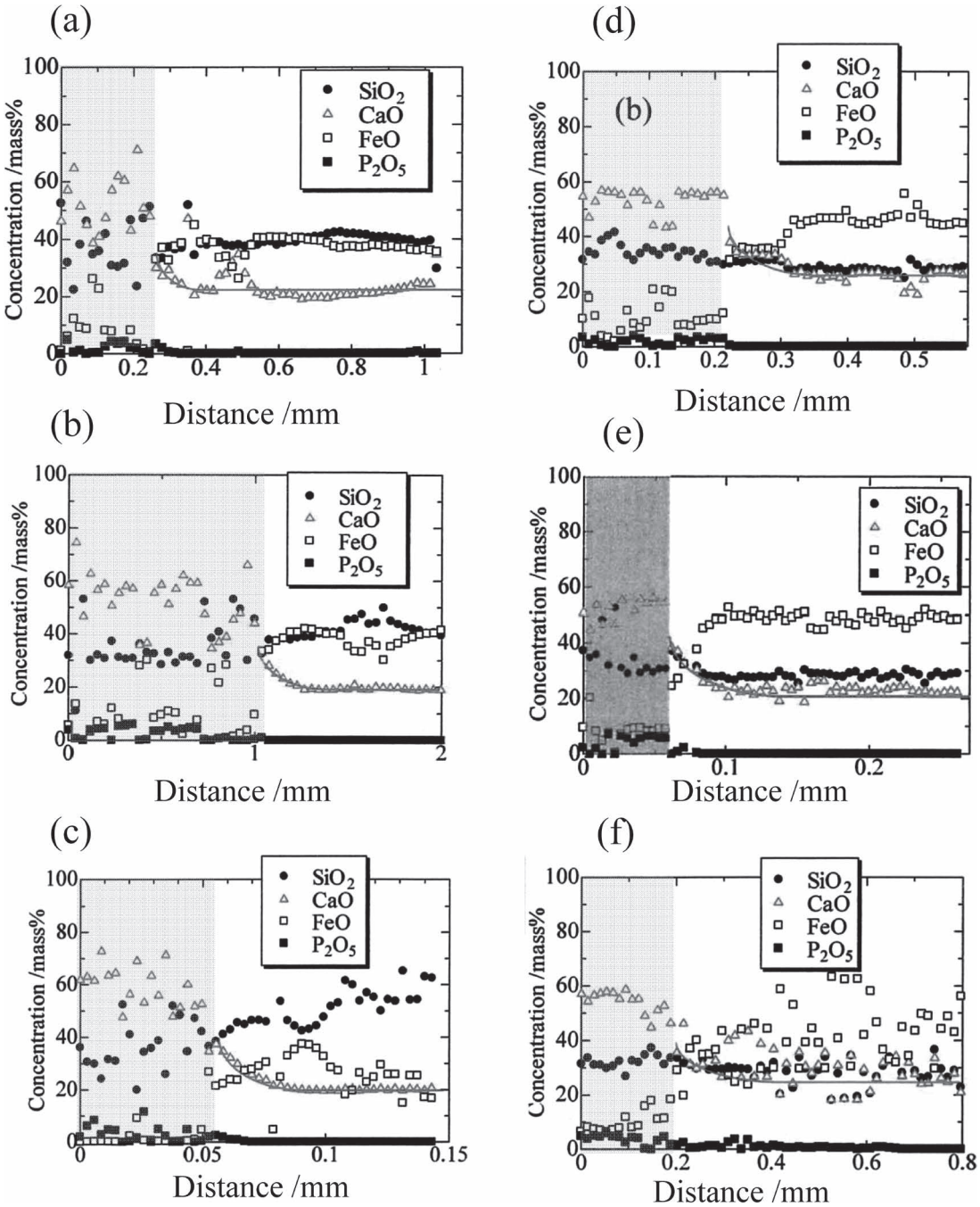

Fig. 6. Concentration profile for the components in the sample of (a) B held for 25 s at 1 573 K, (b) B held for 24 s at 1 623 K, (c) B held for 20 s at 1 673 K, (d) C held for 40 s at 1 573 K, (e) C held for 40 s at 1 623 K, and (f) C held for 40 s at 1 673 K.

3 and D_{CaO} in the slag B at various temperatures listed in **Table 4**, have been determined. Nagata *et al.*[14] reported inter-diffusivities of $D_{CaO-SiO_2}$, D_{SiO_2-FeO} and D_{Fe-CaO} in the slag having the composition of 40CaO-40SiO_2-20FeO on mass% basis to be 4.6×10^{-6}, 7.2×10^{-6} and 8.1×10^{-6} cm^2/s, respectively. The diffusivities obtained in the present study are close to their reported values in the same order, indicating the derivation of diffusivity of the present method would be appropriate.

Temperature dependence of the diffusivity can be evaluated from the data for slags B and C in Table 4. The Arrhenius equation expressed by Eq. (11) is usually applied to evaluate the activation energy for the diffusion;

$$D = D_0 \exp(-Q / RT) \quad \text{..... (11)}$$

Table 3. Diffusivity of CaO and SiO_2 for slags A, C and D at 1 673 K.

	D(CaO)/$cm^2\cdot s^{-1}$	D(SiO_2)/$cm^2\cdot s^{-1}$
Slag A (30%CaO-20%FeO-50%SiO_2)	1.5×10^{-6}	1.5×10^{-6}
Slag C (21.6%CaO-50%FeO-28.4%SiO_2)	1.9×10^{-6}	4.9×10^{-7}
Slag D (13.2%CaO-80%FeO-6.8%SiO_2)	3.3×10^{-5}	4.7×10^{-5}

Relationship between the present diffusivities and reciprocal value of temperature is plotted in **Fig. 7**. This Arrhenius plot gives the activation energy as the slope of linear relation of

Table 4. Diffusivity of CaO for slags B and C at 1 573, 1 623 and 1 673 K.

	D(CaO)/cm^2·s^{-1}	
T/K	Slag B 20%CaO-40%FeO-40%SiO_2	Slag C 21.6%CaO-50%FeO-28.4%SiO_2
1 573	1.64×10^{-6}	1.02×10^{-6}
1 623	3.49×10^{-6}	4.71×10^{-6}
1 673	7.18×10^{-6}	3.31×10^{-6}

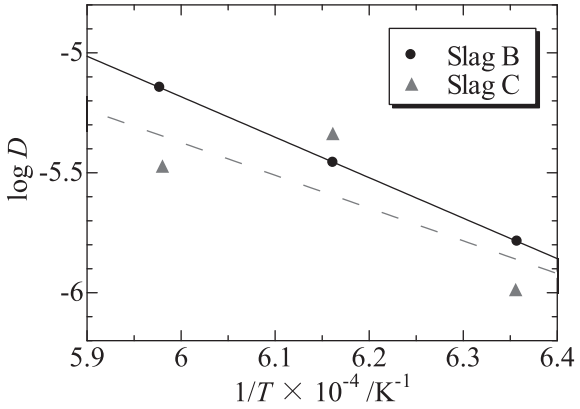

Fig. 7. Relation between diffusivities of CaO and temperature for slags B and C.

Eqs. (12) and (13), which are 323 and 261 kJ/mol for slag B and C, respectively.

$$D = 11.4\times\exp\left(-323/RT\right) \quad \text{..... (12)}$$

$$D = 6.5\times\exp\left(-261/RT\right) \quad \text{..... (13)}$$

It should be noted that the linearity of this relation for slag C is not good enough to apparently hold with Arrhenius relation; thereby, the anticipated linear correlation is shown in a dashed line and the activation energy derived from this linearity for slag C should be considered reference value. However, these activation energies are comparable to the reported value of 235 kJ,[10] proving that temperature dependences obtained are reasonable. In addition, the larger activation energy of slag B would be due to the higher viscosity induced by higher concentration of SiO_2 which is a network forming component.

A kinetic discussion has been made on the complete dissipation time of C2S ball, which simulates the practical dissolution behavior of CaO into the slag assuming that the CaO dissolves by the repeated steps of immediate formation and dissolution of C2S on the surface of CaO. **Figure 8** shows the schematic drawing of dissipation process of C2S ball having the diameter of 1 cm in the slag flow. Assuming that the rate-controlling step of the dissolution is mass transfer in the film boundary on the surface of the sphere, mass flux, J, in the materials balance equation of Eq. (14) is expressed by Eq. (15):

$$4\pi r^2 J = -4\pi r^2 \rho\left(dr/dt\right) \quad \text{..... (14)}$$

$$J = (D/\delta)(C_1 - C_0) \quad \text{..... (15)}$$

Regarding the mass transfer around spherical material,

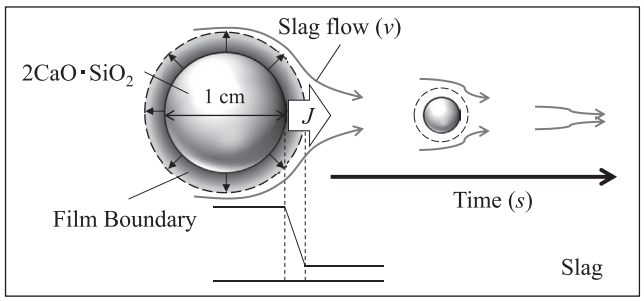

Fig. 8. Schematic diagram of dissolution behavior of C2S ball into the slag.

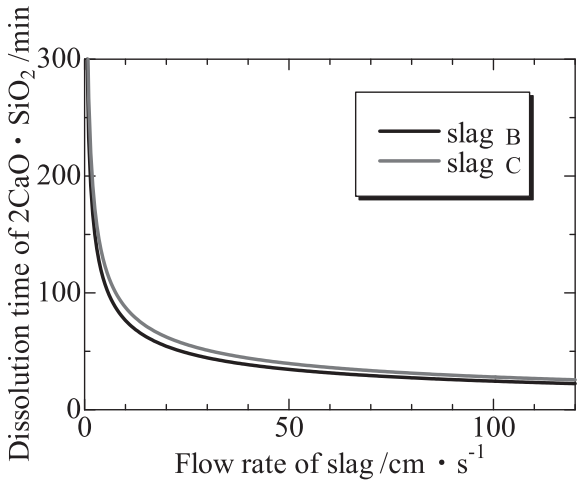

Fig. 9. Relation between dissolution time of C2S and velocity of the slag flow at 1 623 K.

Ranz-Marshall's equation[15] holds which relates Sherwood number (Sh) with Reynolds number (Re) and Schmidt number (Sc) as follows:

$$Sh = 2.0 + 0.6Re^{1/2}Sc^{1/3} \quad \text{..... (16)}$$

According to the definition of these dimensionless numbers, thickness of the film boundary, δ, can be estimated as follows by using the thermo-physical data[12] on the basis of Eq. (16).

$$d/\delta = 2.0 + 0.6\mu^{-1/6}\rho^{1/6}D^{-1/3}v^{1/2} \quad \text{..... (17)}$$

Then, complete dissipation time for a C2S ball having the diameter of 1.0 cm can be calculated for slags B and C as functions of the velocity of the slag flow as shown in **Fig. 9**. Complete dissipation time is too long for the practical refining operation time unless the slag flow rate is as high as several tens cm/s. Only slight difference is found between slags B and C although the FeO concentration is different by about 10 mass%, which seemingly promotes the lime dissolution. The effect of temperature would be worth considering, calculation results of which are shown in **Fig. 10**, where the diffusivity at higher temperature is estimated by the extrapolation by using Eq. (12) and dashed lines are drawn for these cases. Rise in temperature significantly increases dissolution rate leading to remarkable shortening of dissipation time, presumably due to dramatic change in diffusivity and viscosity. Thus, temperature would be more important factor to facilitate the CaO dissolution than slag composition if its change is limited to about 10 mass% as

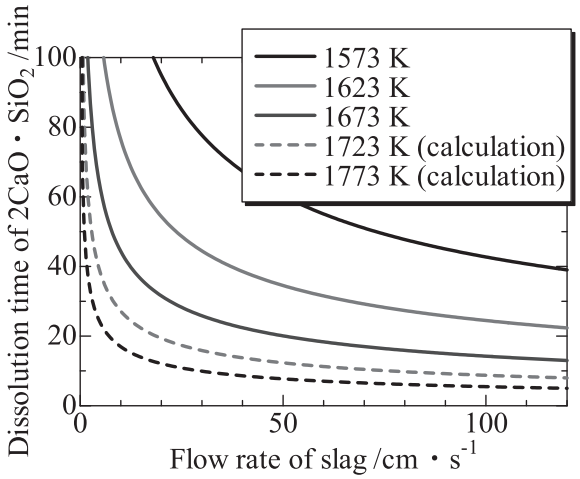

Fig. 10. Change with temperature in relation between dissolution time of C2S and velocity of the slag flow in slag B.

for FeO concentration.

From the viewpoint of kinetics of CaO dissolution, higher temperature is desirable as is mentioned above; however, exothermic reaction of oxidative refining such as dephosphorisation has disadvantage at higher temperature thermodynamically. Therefore, the optimal temperature would exist where both smooth CaO dissolution and effective dephosphorisation are feasible and further practical investigation is expected to make the most of lime fluxing process.

4. Conclusions

Rate of $2CaO{\cdot}SiO_2$ dissolution into molten CaO–FeO–SiO_2 slag has been investigated to promote lime fluxing and conclusions are summarized as follows;

(1) A new diffusion couple method has been established which enables the elucidation of diffusion behavior of solid phase components into liquid phase by suppression of convection in liquid phase.

(2) Diffusivities of CaO and SiO_2 in molten CaO–FeO–SiO_2 slag have been determined to range from 4.9×10^{-7} to 4.7×10^{-5} cm^2/s at temperatures of 1 573 to 1 673 K.

(3) Complete dissipation time of $2CaO{\cdot}SiO_2$ ball into flowing molten slag by dissolution has been estimated and temperature would be the more controlling factor for promotion of lime dissolution.

Acknowledgment

The authors are greatly thankful to Prof. Masahiro Susa and Prof. Rie Endo for their helpful advices and fruitful discussion. We are also much obliged to the Japan Society for the Promotion of Science, 19th Committee, for their financial support to the present research.

Nomenclature

J_i: mass flux of component i ($kg/m^2{\cdot}s$)
M_{ij}: transportation constant ($mol{\cdot}kg/J{\cdot}m{\cdot}s$)
μ_i: chemical potential of component i (J/mol)
x: distance in the direction of diffusion (m)
D: the parameter of inter-diffusion matrix (m^2/s): tabulated on (cm^2/s) basis by convention
C: concentration of the component and t is lapse of time (kg/m^3)
a: radius of cylinder (m)
r: distance from the center of cylinder (m)
C: concentration at distance r (kg/m^3)
C_0: the initial concentration (kg/m^3)
C_1: concentration at C2S saturation (kg/m^3)
J_α: Bessel function of the order of α (dimensionless)
Y_α: Neumann function of the order of α (dimensionless)
D_0: frequency factor (m^2/s)
r: radius of residual sphere (m)
ρ: density (kg/m^3)
δ: thickness of film boundary (m)
d: diameter of C2S ball (m)
δ: thickness of grain boundary (m)
μ: viscosity ($kg/m{\cdot}s$)
v: kinetic viscosity (m^2/s)

REFERENCES

1) M. Matsushima, N. Yadoomaru, K. Mori and Y. Kawai: *Tetsu-to-Hagané*, **62** (1976), 182.
2) T. Hamano, M. Horibe and K. Ito: *ISIJ Int*., **44** (2004), 263.
3) R. Saito, H. Matsuura, K. Nakase, Y. Xiao and F. Tsukihashi: *Tetsu-to-Hagané*, **95** (2009), 258.
4) N. Maruoka, A. Ishikawa, H. Shibata and S. Kitamura: *CAMP-ISIJ*, **25** (2012), 217, CD-ROM.
5) T. Deng, J. Gran and D. Sichen: *Steel Res. Int.*, **81** (2010), 347.
6) T. Kurahashi and K. Goto: *Tetsu-to-Hagané*, **61** (1975), S502.
7) M. Kawakami, K. Nagata, M. Sasabe and K. Goto: *Tetsu-to-Hagané*, **62** (1976), 1159.
8) K. Goto, H. Schmalzried and K. Nagata: *Tetsu-to-Hagané*, **61** (1975), 2794.
9) K. Nagata and K. Goto: *Tetsu-to-Hagané*, **62** (1976), 1777.
10) Y. Ukyo and K. S. Goto: *Metall. Trans. B*, **12B** (1981), 449.
11) Y. Ukyo and K. Goto: *Tetsu-to-Hagané*, **68** (1982), 1981.
12) Slag Atlas, 2nd Ed., ed. by Verein Deutscher Eisenhüttenleute (VDEh), Verlag Stahleisen, Düsseldorf, (1995), 126, 335, 370.
13) J. S. Kirkaldy: *Can. J. Phys*., **35** (1957), 435.
14) K. Nagata, N. Sata and K. Goto: *Tetsu-to-Hagané*, **68** (1982), 1694.
15) W. E. Ranz and W. R. Marshall, Jr.: *Chem. Eng. Prog*., **48** (1952), 173.